

Determining Hubbard *U* of VO_2 by the quasi-harmonic approximation

Longjuan Kong(孔龙娟), Yuhang Lu(陆雨航), Xinying Zhuang(庄新莹), Zhiyong Zhou(周志勇), and Zhenpeng Hu(胡振芃)

Citation: Chin. Phys. B, 2024, 33 (**1**): 016302. DOI: 10.1088/1674-1056/acfd18
Journal homepage: http://cpb.iphy.ac.cn; http://iopscience.iop.org/cpb

What follows is a list of articles you may be interested in

Straight and twisted Weyl nodal line phonons in Ho_2CF_2 material

Xin-Yue Kang(康鑫越), Jin-Yang Li(李金洋), and Si Li(李思)
Chin. Phys. B, 2023, 32 (**11**): 116301. DOI: 10.1088/1674-1056/aceaea

Evaluating thermal expansion in fluorides and oxides: Machine learning predictions with connectivity descriptors

Yilin Zhang(张轶霖), Huimin Mu(穆慧敏), Yuxin Cai(蔡雨欣), Xiaoyu Wang(王啸宇), Kun Zhou(周琨), Fuyu Tian(田伏钰), Yuhao Fu(付钰豪), and Lijun Zhang(张立军)
Chin. Phys. B, 2023, 32 (**5**): 056302. DOI: 10.1088/1674-1056/accdca

Evaluation of performance of machine learning methods in mining structure—property data of halide perovskite materials

Ruoting Zhao(赵若廷), Bangyu Xing(邢邦昱), Huimin Mu(穆慧敏), Yuhao Fu(付钰豪), and Lijun Zhang(张立军)
Chin. Phys. B, 2022, 31 (**5**): 056302. DOI: 10.1088/1674-1056/ac5d2d

Mechanical, electronic, and thermodynamic properties of zirconium carbide from first-principles calculations

Yang Xiao-Yong (杨晓勇), Lu Yong (鲁勇), Zheng Fa-Wei (郑法伟), Zhang Ping (张平)
Chin. Phys. B, 2015, 24 (**11**): 116301. DOI: 10.1088/1674-1056/24/11/116301

Investigations of high-pressure and high-temperature behaviors of the newly-discovered willemite-Ⅱ and post-phenacite silicon nitrides

Chen Dong (陈东)
Chin. Phys. B, 2013, 22 (**12**): 126301. DOI: 10.1088/1674-1056/22/12/126301

Determining Hubbard U of VO_2 by the quasi-harmonic approximation

Longjuan Kong(孔龙娟), Yuhang Lu(陆雨航), Xinying Zhuang(庄新莹), Zhiyong Zhou(周志勇), and Zhenpeng Hu(胡振芃)†

School of Physics, Nankai University, Tianjin 300071, *China*

(Received 18 July 2023; revised manuscript received 22 September 2023; accepted manuscript online 26 September 2023)

Vanadium dioxide VO_2 is a strongly correlated material that undergoes a metal-to-insulator transition around 340 K. In order to describe the electron correlation effects in VO_2, the DFT $+U$ method is commonly employed in calculations. However, the choice of the Hubbard U parameter has been a subject of debate and its value has been reported over a wide range. In this paper, taking focus on the phase transition behavior of VO_2, the Hubbard U parameter for vanadium oxide is determined by using the quasi-harmonic approximation (QHA). First-principles calculations demonstrate that the phase transition temperature can be modulated by varying the U values. The phase transition temperature can be well reproduced by the calculations using the Perdew–Burke–Ernzerhof functional combined with the U parameter of 1.5 eV. Additionally, the calculated band structure, insulating or metallic properties, and phonon dispersion with this U value are in line with experimental observations. By employing the QHA to determine the Hubbard U parameter, this study provides valuable insights into the phase transition behavior of VO_2. The findings highlight the importance of electron correlation effects in accurately describing the properties of this material. The agreement between the calculated results and experimental observations further validates the chosen U value and supports the use of the DFT $+U$ method in studying VO_2.

Keywords: quasi-harmonic approximation, vanadium dioxide, first-principles calculation, Hubbard U

PACS: 63.20.dk, 63.22.–m, 63.20.D–, 71.10.Fd **DOI:** 10.1088/1674-1056/acfd18

1. Introduction

Strongly correlated transition metal oxides exhibit a wide range of intriguing physical properties, including magnetoresistance, superconductivity, and metal–insulator transition (MIT), which arise from their strong electron–electron correlation effects.[1–6] These materials have attracted significant attention in recent years and hold great potential for various applications.[7–11] Among them, vanadium dioxide VO_2 stands out as a representative material that has been extensively studied due to its remarkable feature known as the metal-to-insulator transition.[12] This transition was first discovered by Morin in 1959 and occurs around 340 K, accompanied by a simultaneous structural change from the high-temperature conducting rutile (R) phase to the low-temperature insulating monoclinic (M) phase, with a band gap of approximately 0.6 eV.[12–14] The MIT of VO_2 near room temperature is associated with rapid changes in its structural, electrical, optical, thermal, and magnetic properties.[15–19] The reversible nature of this transition, along with the relative ease of synthesis,[20–23] makes VO_2 an ideal material for various applications, including smart windows,[24,25] photoelectric switches,[26] information storage,[27] and thermal control of spacecraft.[28] Moreover, the unique MIT behavior of VO_2 has gained renewed attention with the development of new ultrafast microscopy techniques.[29,30] The MIT in VO_2, with its drastically changed physical properties, can be triggered by different stimuli such as temperature, pressure, light, electric field, and doping.[31,32]

Furthermore, VO_2 not only provides a playground for exploring the peculiar MIT and corresponding applications, but paves the way for tackling strongly correlated systems. Unfortunately, the precise elucidation of the physical properties of materials with strongly correlated electronic behavior has continued to be a challenging subject in condensed matter physics. An inexpensive and reliable way to evaluate the physical features of with strong correlated d/f electrons is the calculations based on or beyond the density functional theory (DFT). As a consequence, extensive theoretical works have been performed, including but not limited to classical DFT within the local density approximation (LDA),[33,34] and the generalized gradient approximation (GGA),[35] hybrid functions,[36] GW (G refers to Green's function and W denotes the dynamically screened Coulomb interaction),[37] and dynamical mean field theory (DMFT).[38] It is noticed that LDA and GGA cannot describe the electronic structure of M-VO_2 correctly. The GW approximation and the random phase approximation (RPA) have been proved rather useful to describe the excitation of materials. The DMFT may correctly describe the electronic properties of both R and M phases of VO_2. Unfortunately, these three methods fall short for the calculations of forces and suffer from the high computational cost. Though hybrid functional may be used to calculate forces, it still suffers from the high computational cost and fails in describing the metallic behavior of R-VO_2.[39] Generally, the DFT $+U$ method is

†Corresponding author. E-mail: zphu@nankai.edu.cn

© 2024 Chinese Physical Society and IOP Publishing Ltd

tuned to be extensively used to study ground state properties such as structural, electronic and thermal properties with an economic computational cost. The strong electron–electron Coulomb interaction in the 3d orbital of VO_2 and the drastic change in electrical conductivity following MIT make this system can be studied using Hubbard model with the consideration of U parameter. [40] Taking Hubbard U as an adjustable parameter, DFT + U method is easy to reproduce the nature of VO_2, and it is suitable to calculate the total energy, atomic force, and stress accurately. These physical quantities, including the phase transition, mechanical properties, characteristics of surface and interface, and chemical reactions, are essential for better understanding of the richness of VO_2. Usually, the conventional DFT, adding a Hubbard U parameter representing the strong electron–electron interaction of strongly correlated materials, can cure the deficiencies of local or semi-local exchange-correlation functions and maintain relatively low computational cost.[41–43]

As was reported, the accuracy of outcomes by DFT + U is tend to depend on the magnitude of U parameter. In the need of the correct description of strongly correlated system properties, it is necessary to determine a reliable U value firstly. Hence, many methods have been proposed to determine the optimal U value. The widely used approach reported in literature for choosing effective U is adjusting calculated results to fitting experimental data (for instance, fitting the experimental bandgaps, seeback effect or electrical conductivity).[42,44,45] On the other hand, several pure theoretical perspectives have also been developed to determine the U non-empirically, for example, the linear response method based on constrained DFT (CDFT) by Cococcioni and de Gironcoli1,[46] the constrained random-phase approximation (cRPA) method,[47] and self-consistent methods from the local electron density based on the Thomas–Fermi screening mode.[48] However, these methods have shortcomings more or less. For example, the limitation of determining Hubbard U by fitting the experimental band gap data may lead to a huge U in some materials, which is a lack of physical meaning. Meanwhile, several pure theoretical methods may either suffer significant expensive computation and fall short for Hellmann–Feynman force calculations,[37,49] or fail to obtain the effective U value correctly describing two VO_2 phases simultaneously.[50] Considering the efficiency and accuracy, the effective U value can also be indirectly appreciated by the comparing calculated phase transition temperature T_c based on quasi-harmonic approximation (QHA) with that of experiment, from the thermodynamical aspect during MIT process. Actually already in 2014, Budai *et al*. provided a full thermodynamic understanding the nature of VO_2 MIT by using x-ray and neutron scattering margins, revealing the importance of anharmonic phonons of lattice vibrations in phase-transition process.[51] The QHA, which takes into part of the anharmonic effects, may be a much more straightforward and computationally cheap method used to investigate thermodynamics properties, including the thermal expansion coefficients, the heat capacities, vibration entropy, and free energy.

In this paper, we propose a method to determine the optimal Hubbard U value of VO_2 based on the transition temperature T_c using the QHA from a thermodynamic perspective. We demonstrate that the obtained U value is highly effective in capturing the correct physical properties of both the monoclinic (M) and rutile (R) structures of VO_2. Focusing on the metal-to-insulator transition of vanadium dioxide, we choose to fit the phase transition temperature to determine the Hubbard U in DFT + U calculations with the quasi-harmonic approximation. Different U values have been evaluated for the properties of either monoclinic or rutile phase, including structural information, band structure, as well as the phase transition temperature. After considering the electronic part of free energy, the U of 1.5 eV is proved to be an optimal one for Perdew–Burke–Ernzerhof (PBE) + U calculations of VO_2. It can well reproduce the essential properties of VO_2, which is efficient in the calculations. Overall, our method provides a reliable approach for determining the appropriate U value in DFT + U calculations of strongly correlated materials like VO_2.

2. Theoretical methods and computational details

In this work, we performed the geometrical optimization and electronic properties' calculations under the framework of density functional theory, as implemented in the Vienna *ab initio* simulation package (VASP).[52,53] The projector augmented-wave (PAW)[54] pseduo potential was employed to describe the interaction between the core and valence electrons. The exchange–correlation interaction was described by the PBE functional.[55] The electron wavefunction was expanded in a plane-wave basis set with an energy cutoff of 520 eV. In order to ensure a reliable energy comparison between two VO_2 phases, a reciprocal-grid density of $\approx \frac{60}{a} \times \frac{60}{b} \times \frac{60}{c}$ was used, where a, b, and c are the lattice constants in units of angstrom. Then, the k-point grids of $9 \times 11 \times 9$ and $12 \times 12 \times 20$ were determined for M and R cells, respectively. Since the previous studies have shown that the physical properties of strongly correlated system depend significantly on the magnitude of U, we rationally tested different Hubbard U values. The convergence criteria for force and energy are 10^{-3} eV/Å and 10^{-8} eV, respectively.

The PHONOPY software[56,57] was employed to calculate the phonon related information at harmonic and quasi-harmonic levels, including phonon dispersion, vibration free energy, the heat capacity, Helmholtz free energy, and the

Gibbs free energy. The force constants of the supercell including 48 atoms for either M or R phase were calculated through the density-functional perturbation theory (DFPT).[58] A mesh grid of $40\times40\times40$ q-points was generated to make calculation more accurate.

The finite temperature-dependent physical quantities were obtained by using the QHA,[56,59] including vibration free energy, the heat capacity, Helmholtz free energy, and the Gibbs free energy. The temperature was assumed to indirectly affect phonon frequencies through thermal expansion and temperature dependence of phonon frequencies. Within the QHA, the Helmholtz free energy of a crystal is expressed as

$$F(V,T)=E_{\text{static}}(V,0\text{ K})+E_{\text{zpe}}(V,0\text{ K})-F_{\text{ph}}(V,T), \quad (1)$$

where $E_{\text{static}}(V,0\text{ K})$ is the first-principles zero-temperature energy of a static lattice at volume V. The second term in Eq. (1), $E_{\text{zpe}}(V,0\text{ K})$, is the zero-point energy that can be written as

$$E_{\text{zpe}}(V,0\text{ K})=\frac{1}{2}\sum_{i,\boldsymbol{q}}\hbar\omega_{i,\boldsymbol{q}}(V). \quad (2)$$

The last term is the phonon free energy due to lattice vibration, given by

$$F_{\text{ph}}(V,T)=k_{\text{B}}T\sum_{i,\boldsymbol{q}}\ln\{1-\exp[-\hbar\omega_{i,\boldsymbol{q}}(V)/(k_{\text{B}}T)]\}, \quad (3)$$

where $\omega_{i,\boldsymbol{q}}(V)$ is the volume-dependent vibrational frequency of i-th mode at wavevector $\boldsymbol{q}$, k_{B} and $\hbar$ are the Boltzmann and the reduced Planck constant, respectively. Hence the vibrational entropy can be obtained by

$$\begin{aligned}S_{\text{vib}}&=-\left(\frac{\partial F_{\text{ph}}}{\partial T}\right)_V\\&=-k_{\text{B}}\sum_{i,\boldsymbol{q}}\ln\left\{1-\exp[-\hbar\omega_{i,\boldsymbol{q}}(V)/(k_{\text{B}}T)]\right\}\\&\quad-\frac{1}{T}\sum_{i,\boldsymbol{q}(V)}\frac{\hbar\omega_{i,\boldsymbol{q}(V)}}{\exp[\hbar\omega_{i,\boldsymbol{q}}(V)/(k_{\text{B}}T)]-1}.\end{aligned} \quad (4)$$

Then the heat capacity can be calculated from vibrational entropy

$$\begin{aligned}C_V&=T\left(\frac{\partial S_{\text{vib}}}{\partial T}\right)_V\\&=k_{\text{B}}\sum_{i,\boldsymbol{q}}\left[\frac{\hbar\omega_{i,\boldsymbol{q}}(V)}{k_{\text{B}}T}\right]^2\frac{\exp[\hbar\omega_{i,\boldsymbol{q}}(V)/(k_{\text{B}}T)]}{\{\exp[\hbar\omega_{i,\boldsymbol{q}}(V)/(k_{\text{B}}T)]-1\}^2}.\end{aligned} \quad (5)$$

The Helmholtz free energies $F(V,T)$ shown in Eq. (1) were calculated at 9 volume points of each specified temperature. Furthermore, the Vinet equation of state was used to fit the nine of $F(V,T)$ at each T variable within a specified temperature window considered, and the equilibrium volume at each T was obtained corresponding to the minimum value of fitted curve. The Gibbs free energy as a function of temperature/pressure can be written as

$$G(p,T)=F(V(p,T),T)+pV(p,T), \quad (6)$$

where $p=\partial E/\partial V\approx0$ under the atmosphere. Transition temperature can be obtained by tracking and comparing Gibbs free energies of M and R phases as a function of temperature, satisfying Eq. (6). When Gibbs free energies of R and M phases are equal, the transition occurs naturally and the T_{c} can be obtained simultaneously.

3. Results and discussion

3.1. Structural properties and band gap

At a temperature below T_{c}, the VO_2 is a monoclinic (M) structure with space-group $P2_1/c$ (No. 14) with the unit cell parameters of $a\approx5.388$ Å, $b\approx4.614$ Å, $c\approx5.441$ Å. The V^{4+} ions deviates from the vertex and center of the unit cell, which results in the twist VO_6 octahedral cages as basic building blocks (shown in the left part of Fig. 1(a)). Another feature of M phase is that the vanadium atoms title and dimerize to form zigzag-like chains with alternating different V–V bond distances, as shown in right panel of Fig. 1(a). As shown in Fig. 1(b), at ambient pressure and above T_{c}, the thermodynamically stable phase of VO_2 belongs to the $P4_2/mnm$ (No. 136) space group with tetragonal rutile (R) structure. It has the lattice constants of $a=b\approx4.627$ Å, $c\approx2.797$ Å. In the R-VO_2 phase, the V^{4+} ions occupy the apex and body center of the tetragonal crystal cell, and six O^{2-} ions surrounding one V^{4+} ion constitute an octahedral VO_6 unit (see the left panel of Fig. 1(b)). In addition, the octahedral unit forms edge-sharing chains along the c axis. As illustrated in right panel of Fig. 1(b), vanadium atoms form equally spaced V–V straight chains in c direction.

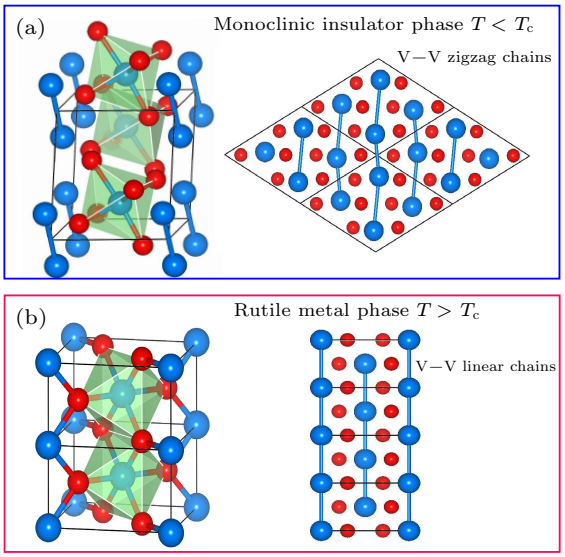


Fig. 1. Crystal structure of VO_2 in (a) monoclinic (M) phase with alternating V–V dimerization forming zigzag-like chains and (b) rutile (R) phase with equidistant straight V–V chains. The unit cells are indicated by black lines. Vanadium and oxygen atoms are represented by blue and red spheres, respectively.

Table 1. Band gaps and V–V distances of M and R phases by DFT + U with different U values, and compared with the experimental results.

Hubbard U (eV)	M-VO_2		R-VO_2	
	V–V distance (Å)	Band gap (eV)	V–V distance (Å)	Band gap (eV)
1	2.50	3.19	2.80	metal
2		0.21		
3		0.44		
4		0.71		
Experimental	2.62[60]	3.16[34]	2.85(360 K)[61]	
		0.67[13]		

As described above, one of the distinguishing features of VO_2 is its strongly correlated 3d electrons. Although the periodic plane-wave DFT calculations with typical exchange-correlation functions, such as LDA or GGA, have significant success in describing many materials, they fail to treat strongly correlated systems. Usually, they may underestimate the band gaps and sometimes even predict qualitatively incorrect metallic ground state, e.g., insulating nature M-VO_2. This discrepancy is mainly due to inaccurate treatment of electron correlation effects. Therefore, in order to overcome this shortcoming, the DFT + U method with a moderate computational cost was used in the present work to better understand the electronic properties of two VO_2 phases. The strong Coulomb interactions between V-3d electrons are represented by the Hubbard U parameter. In the case of M-VO_2, the band should open a reliable gap and restore insulating character. However, previous studies have shown that the calculation results depend on the magnitude of effective U values, so we systematically examined the effects of different U values on band gaps. Here, we mainly focus on the effect of Hubbard U parameter on electronic structure rather than the geometrical structure. Hence, the V–V distances for the two phases shown in Table 1 are obtained from the fully optimized crystal structures by the PBE function without considering the Hubbard U parameter. The PBE function can correctly reproduce two different dimerized V–V bond distances for the monoclinic phase (2.50 Å and 3.19 Å compared to the experimental values 2.62 Å and 3.16 Å, respectively). In the rutile phase, the optimized equal V–V bond length is $\sim$ 2.80 Å, which is close to the experimentally reported value of 2.85 Å. Taking U as the adjustable parameter in a range between 1 eV and 4 eV, the DFT + U results reproduce the insulating nature of M phase. The band gaps are 0.21 eV, 0.44 eV, 0.71 eV, and 1.00 eV with $U = 1$ eV, 2 eV, 3 eV, 4 eV, respectively. It shows a positive correlation between the band gaps and the U values. Meanwhile, the metallic character of R structure is preserved. From these results, we may speculate that the tuning U in the region of 2–3 eV may be required to match the optical gap (0.67 eV) from the experiments. However, one should remember that the experimental gap is measured by photoemission in an exciting progress, in which the interacting electron–hole pair is also included. A good agreement between calculation and experiment can only be achieved by considering the excitonic effects, especially in the case that there is a semiconductor or an insulator. The Bethe–Salpeter equation under the GW approximation (GW-BSE) may be appropriate for this process, but it makes the calculation expensive and cumbersome. Therefore, we would like to use a relatively inexpensive DFT + U method to capture the correct qualitative features of VO_2 system in the present work, where the reliable V–V bonds for both the phases and a finite band gap of M phase (but not the same value as the experimental one) should be reproduced.

3.2. Phonon dispersion and phase transition temperature

According to the workflow of QHA method, the phonon spectra based on force constants obtained by the density-functional perturbation theory (DFPT) are required prior to the actual thermodynamically physical quantities calculation. For instance, the $\omega_{i,\boldsymbol{q}}$ is used to calculate zero-point energy and free energy of lattice vibration, as seen on the right-hand sides of Eqs. (2) and (3). Hence, we have first calculated the phonon dispersion curves for both M-VO_2 and R-VO_2 using DFT + U with $U = 1$ eV (Fig. 2). In a cell with n-atoms, there would be 3 acoustic branches, $3n-3$ optical branches. There are 36 and 18 branches in the primitive cells of M and R phases, respectively. As shown in Figs. 2(a) and 2(b), there is no imaginary frequency existing in the whole Brillouin zone for both the phases. It provides a direct proof of their dynamical stability under the simulated condition. From the projected phonon density of states of both the phases shown in Fig. 2, the low frequency part is mainly contributed by V atoms (black solid line), and the high frequency is mainly originated from O atoms (red solid line). In addition, V atoms is more dominant for phonon modes with frequencies lower than 5 THz. These results are in agreement with the other phonon calculations given by Lee *et al.*[62] For the R phase, our results are different with the results from Hua *et al.*,[63] where there were a lot of imaginary frequencies without considering a Hubbard U. This difference highlights the necessity of considering the correlation effect in rutile phase VO_2. Additionally, the three non-degenerated acoustic branches, one longitude and two transverse branches, indicated that M and R phases are both anisotropic. The phonon dispersion curves by DFT + U with other U values were also calculated. Though the details may vary slightly, there is no imaginary frequency in phonon spectra for the two phases. To keep the present text succinct,

only the results of $U = 1$ eV is presented in Fig. 2.

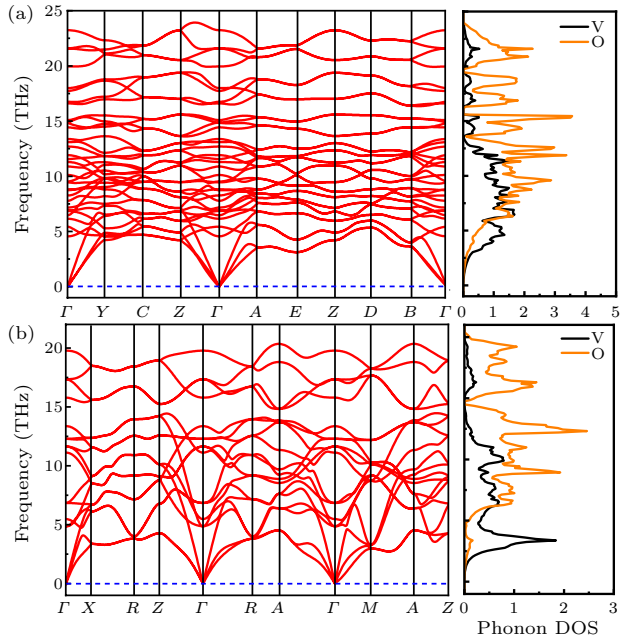


Fig. 2. Phonon dispersion along high symmetry lines and the phonon density of states for VO_2 in (a) M phase and (b) R phase.

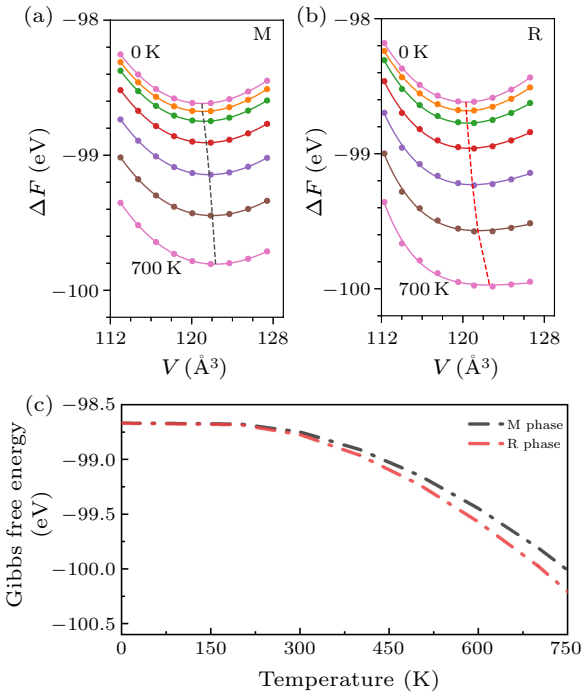


Fig. 3. Helmholtz free energy with respect to different volumes of VO_2 in (a) M phase and (b) R phase at temperature window between 0 and 700 K with steps of 100 K. The filled circles denote calculated Helmholtz free energy with QHA of nine volumes at specified temperature, and the solid curves show the fitted functions according to the Vinet equation of states. The crossed points of solid and dashed line are the minimum of respective fitted functions and simultaneously represent the equilibrium volumes at each temperature. Dashed lines are a guide to the eyes. (c) The Gibbs free energies of varied temperatures for M and R phases, evolving from the dashed lines in (a) and (b), respectively.

The thermodynamic properties are calculated consequently, including the entropy, free energy, heat capacity, and so on. Figures 3(a) and 3(b) show the volume-dependent quasi-harmonic Helmholtz free energies of M and R phases. The free energies as a function of lattice cell volume at each specified temperature from 0 K to 700 K with a step of 100 K calculated with QHA for $U = 1.0$ eV are depicted by filled circles. These calculated points are fitted by the Vinet equation of states (EOS)[64] to get the equilibrium volumes at different temperatures. As shown in Figs. 3(a) and 3(b), using QHA makes it possible to preserve part of the finite temperature effect caused by the changes of phonon frequencies with the increase in equilibrium lattice volume at different temperatures. Within the framework of the QHA, the Gibbs free energy at given temperatures and a certain pressure can be obtained (the crossed points of black or red dashed line and colored solid lines). The Gibbs free energy of both M and R phases as functions of temperatures are presented in Fig. 3(c). It is well known that the Gibbs free energies of the two phases at the transition point are equal. Therefore, the transition temperature T_c can be evaluated from the cross point of two Gibbs free energy curves. However, from Fig. 3(c) we can find that the Gibbs free energy of R-VO_2 is always lower than that of M-VO_2 in the whole temperature window, which is counter-intuitive and no obvious T_c. This issue may be due to the irrationally selected Hubbard $U = 1.0$ eV, which is inadequate to correct electron–electron strongly correlated interactions.

Keep the above results in mind, one may expect to enhance the T_c by adjusting the U parameter. We thus go one step further to obtain the Gibbs free energy with $U = 2.0$ eV. As illustrated in Fig. 4(a), the Gibbs free energy of M phase is lower than that of R phase in the region of 0–552.1 K, which implies that the M phase is more stable than the R phase and the phase transition occurs at 552.1 K. However the T_c is higher than the experimental data.[12] Although the cross point leftwards with the decreasing Hubbard U to 1.5 eV, the $T_c \approx 396.8$ K [Fig. 4(b)] slightly deviates from the measured value of ~ 340 K. Additionally, the other contributions to the free energy in Eq. (1) should be considered to adjust the T_c further. As is well known, the temperature-dependent electronic energy $E_{\rm elec}(V,T)$ [Eq. (7)], usually ignored for semiconductors, should be emphasized in metal.[65] Further calculations show that the Gibbs free energy of R phase cannot be correctly describe without taking into account the electronic energy (~ 0.14 eV error in 0–1000 K). The reason of this issue is attributed to the large density states at Fermi level of R phase, which yields a substantial contribution of the electronic entropy. Substituting $E_{\rm elec}(V,T)$ for $E_{\rm static}(V,0\ {\rm K})$ in Eq. (1), the modified Gibbs energies of both the phases are shown in Figs. 4(c) and 4(d). The substantial contribution of the electronic entropy ($S_{\rm elec}$) decreases the free energy of R phase and hence induces the reduction of T_c. It is noticed that the phase transition temperature is 347.9 K with the U value of 1.5 eV (Fig. 4(d)). The effective Hubbard U is determined to be 1.5 eV by successfully fitting phase transition temperature.

$$E_{\rm elec}(V,T) = E_{\rm static}(V,0\ {\rm K}) - TS_{\rm elec}. \tag{7}$$

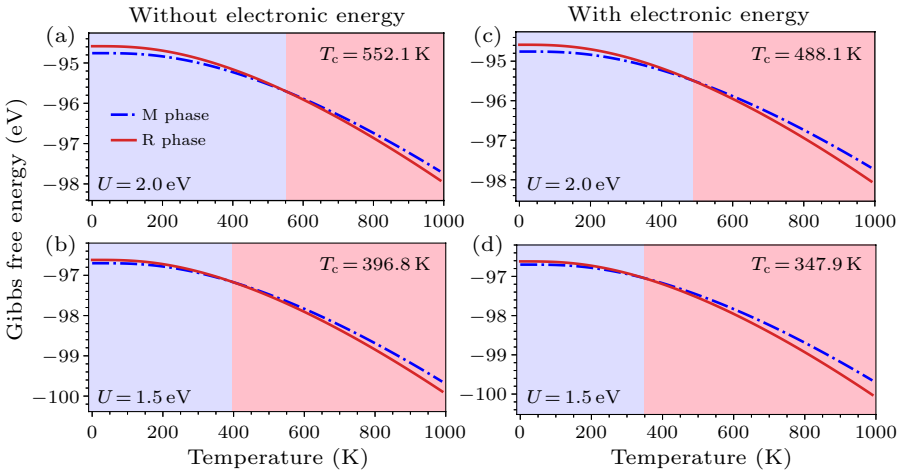


Fig. 4. The Gibbs free energy versus temperature, which is performed in a simpler and efficient framework of DFT + U combined with QHA for both M (blue dashed lines) and R phases (red solid lines) at (a) $U = 2.0$ eV and (b) $U = 1.5$ eV without considering electronic energy in Helmholtz free energy, (c) $U = 2.0$ eV and (d) $U = 1.5$ eV with electronic energy in Helmholtz free energy. The boundary of blue and red shaded region denotes the transition point from low-temperature M phase to high-temperature R phase. The corresponding temperature of boundary is the T_c, as shown in the upper right.

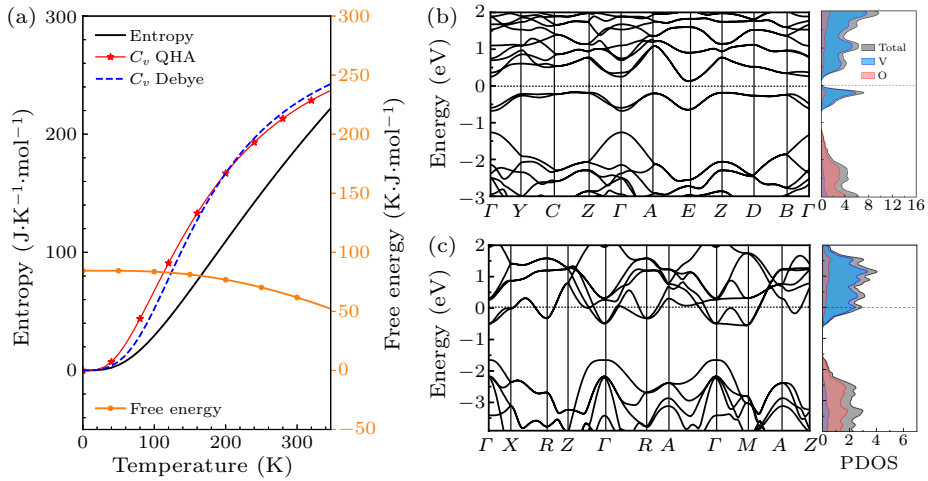


Fig. 5. The calculated thermal properties using DFT + U combined with QHA at $U = 1.5$ eV, including Helmholtz free energy, heat capacity, and entropy for M phase with respect to temperature, shown by orange filled circles, with red filled stars, and black solid line, respectively. The orange and red solid lines connecting filled symbols are guides for the eyes. The blue dashed line denotes the fitted heat capacity as a function of temperature by Debye approximation. Band structures and corresponding partial density of states (PDOS) calculated by DFT + U with $U = 1.5$ eV for (b) M phase and (C) R phase of VO_2. Black dashed line depicts the Fermi level.

3.3. Thermal properties and band structures with determined U

In practice, an optimal Hubbard U value is available to correctly describe fundamental properties of both the VO_2 phases. In order to check the efficiency and reliability of the determined U mentioned above, we choose to examine the thermal properties of M-VO_2 and the electronic band structures of both the phases with the U value of 1.5 eV as the examples. The calculated temperature-dependent free energy, heat capacity and entropy are obtained and presented in Fig. 5(a). The heat capacity C_V simulated by the quasi-harmonic approximation (the red filled stars with guided line in Fig. 5(a)) can be fitted according to the following equation deducted from the Debye approximation:

$$\frac{C_V}{nR} = 9\left(\frac{T}{T_D}\right)^3 \int_0^{T_D/T} \frac{x^4 \cdot e^x}{(e^x - 1)^2} dx. \quad (8)$$

The parameter T_D is fitted to be 728.4 K, agreeing with the experimental value of 750 K.[66] This good agreement provides a direct proof that the QHA method and the U parameter determined by T_c demonstrate the good performance for evaluating thermal properties of VO_2. The electronic band structures of both the M and R phases are also presented in Figs. 5(b) and 5(c) to further verify the efficiency of the determined U. Obviously, the energy zero is shifted to the Fermi energy position in both the figures. The DFT + U with $U = 1.5$ eV give a ~ 0.3 eV indirect band gap for the insulating M phase, and characterizes the metal nature of R phase. The shapes of band curves near Fermi level are comparable to the previous DFT results.[34,49] The partial density of states (PDOS) shown in the right panel of Figs. 5(a) and 5(b) provide more clear evidence of the instinct characteristic of M phase and R phase. As shown in the right panel of Fig. 5(b), the partial density of states of monoclinic VO_2 is separated

near the Fermi level by a gap of ~ 0.3 eV, which agrees with the property of its band structure discussed above. The top of valence-band sates predominantly is made up of V atoms contributions, while significant components from V atoms also contribute mainly to the lower conduction-band states. The PDOS of rutile VO_2 is shown in the right part of Fig. 5(b). It can be noticed that Fermi level is located in the conduction bands, which indicates the metallic nature of R phase. The lower group of states below the energy -1.5 eV is mainly originated from the O atoms. The states crossing the Fermi level in the energy ranges between -0.5 eV and 2 eV are dominated by the states of vanadium atoms. It should be kept in mind what really matters is the nature of insulating M phase and metallic R phase, but not the exact value band gap. One cannot expect that the electronic band gap of the ground state always matches with the optical gap, especially in the strong correlated materials. In a word, the magnitude of the resulting U determined by T_c based on QHA is physically reliable.

4. Conclusions

Using first-principles calculations with the quasi-harmonic approximation, the temperature-dependent Gibbs free energy curves of insulating M phase and metallic R phase of VO_2 with a certain Hubbard U can be plotted. The transition temperature T_c is determined by identifying the cross point of Gibbs free energy curves during the phase transition. By comparing the calculated T_c with the experimental reference value, the effective Hubbard U value is turned out to be 1.5 eV for VO_2. Moreover, the calculations with this U value may correctly capture the metallic and insulating properties of the M and R phases, respectively. In conclusion, this work demonstrates that the first-principles calculations in combination with QHA can be used to determine the effective Hubbard U value of VO_2 by analyzing the phase transition temperature T_c. This approach is promising for determining U of other strongly correlated materials.

Acknowledgments

This work was supported by the National Natural Science Foundation of China (Grant Nos. 21933006 and 21773124) and the Fundamental Research Funds for the Central Universities Nankai University (Grant Nos. 010-63233001, 63221346, 63213042, and ZB22000103). K.L. acknowledges the support from the China Postdoctoral Science Foundation (Grant No. 2021M691674) and the Hefei National Laboratory for Physical Sciences at the Microscale (Grant No. KF2020105).

References

[1] Dagotto E 2005 *Science* **309** 257
[2] Wu J, Lynn J W, Glinka C J, Burley J, Zheng H, Mitchell J F and Leighton C 2005 *Phys. Rev. Lett.* **94** 037201
[3] Keimer B, Kivelson S A, Norman M R, Uchida S and Zaanen J 2015 *Nature* **518** 179
[4] Lee P A, Nagaosa N and Wen X G 2006 *Rev. Mod. Phys.* **78** 17
[5] Stewart G R 2011 *Rev. Mod. Phys.* **83** 1589
[6] Kim S Y, Lee M C, Han G, Kratochvilova M, Yun S, Moon S J, Sohn C, Park J G, Kim C Y and Noh T W 2018 *Adv. Mater.* **30** 1704777
[7] Hu P, Hu P, Vu T D, Li M, Wang S, Ke Y, Zeng L, Mai L and Long Y 2023 *Chem. Rev.* **123** 4353
[8] Li Y, Zhu Y, Wang M, Zhao M, Xue J, Chen J, Wu T and Chambers S A 2022 *Adv. Funct. Mater.* **32** 2203491
[9] Wang L, Li H, Zhang W, Zhao X, Qiu J, Li A, Zheng X, Hu Z, Si R and Zeng J 2017 *Angew. Chem. Int. Ed.* **56** 4712
[10] Xu X, Xiong F, Meng J, Wang X, Niu C, An Q and Mai L 2020 *Adv. Funct. Mater.* **30** 1904398
[11] Mounasamy V, Mani G K and Madanagurusamy S 2020 *Mikrochim. Acta* **187** 1
[12] Morin F J 1959 *Phys. Rev. Lett.* **3** 34
[13] Cavalleri A, Rini M, Chong H H W, Fourmaux S, Glover T E, Heimann P A, Kiefferand J C and Schoenlein R W 2005 *Phys. Rev. Lett.* **95** 67405
[14] Shin S, Suga S, Taniguchi M, Fujisawa M, Kanzaki H, Fujimori A, Daimon H, Ueda Y, Kosuge K and Kachi S 1990 *Phys. Rev. B* **41** 4993
[15] Berglund C N and Guggenheim H J 1969 *Phys. Rev.* **185** 1022
[16] Savo S, Zhou Y, Castaldi G, Moccia M, Galdi V, Ramanathan S and Sato Y 2015 *Phys. Rev. B* **91** 134105
[17] Kasrga T S, Sun D, Park J H, Coy J M, Fei Z, Xu X and Cobden D H 2012 *Nat. Nanotechnol.* **7** 723
[18] Kats M A, Blanchard R, Zhang S. Genevet P, Ko C, Ramanathan S and Capasso F 2013 *Phys. Rev. X* **3** 041004
[19] Wu C, Zhang X, Dai J, Yang J, Wu Z, Wei S and Xie Y 2011 *J. Mater. Chem. A* **21** 4509
[20] Kang L, Gao Y and Luo H 2009 *ACS Appl. Mater. Interfaces* **1** 2211
[21] Gao Y, Luo H, Zhang Z, Kang L, Chen Z, Du J, Kanehira M and Cao C 2012 *Nano Energy* **1** 221
[22] Vu T D, Chen Z, Zeng X, Jiang M, Liu S, Gao Y and Long Y 2019 *J. Mater. Chem. C* **7** 2121
[23] Li M, Magdassi S, Gao Y and Long Y 2017 *Small* **13** 1701147
[24] Zhang Z, Zhang L, Zhou Y, Cui Y, Chen Z, Liu Y, Li J, Long Y and Gao Y 2023 *Chem. Rev.* **123** 7025
[25] Manning T D, Parkin I P, Pemble M E, Sheel D and Vernardou D 2004 *Chem. Mater.* **16** 744
[26] Soltani M, Chaker M, Haddad E and Kruzelesky R 2006 *Meas. Sci. Technol.* **17** 1052
[27] Lei D Y, Appavoo K, Ligmajer F, Sonnefraud Y, Haglund J R F and Maier S A 2015 *ACS Photon.* **2** 1306
[28] Haddad E, Kruzelecky R V, Murzionak P, Jamroz W, Tagziria K, Chaker M and Ledrogoff B 2022 *Front. Mater.* **9** 1013848
[29] Xu C, Jin C, Chen Z, Lu Q, Cheng Y, Zhang B, Qi F, Chen J, Yin X, Wang G, Xiang D and Qian D 2023 *Nat. Commun.* **14** 1265
[30] Li J, Wu L, Yang S, Jin X, Wang W, Tao J, Boatner L, Babzien M, Fedurin M, Palmer M and Zhu Y 2022 *Phys. Rev. X* **12** 021032
[31] Hattori A N, Osaka A I, Hattori K, Naitoh Y, Shima H, Akinaga H and Tanaka H 2020 *Crystals* **10** 631
[32] Ke Y, Wang S, Liu G, Li M, White T J and Long Y 2018 *Small* **14** 1802025
[33] Wentzcovitch R M, Schulz W W and Allen P B 1994 *Phys. Rev. Lett.* **72** 3389
[34] Eyert V 2002 *Ann. Phys.* **514** 650
[35] Zhu Z and Schwingenschlogl U 2012 *Phys. Rev. B* **86** 075149
[36] Eyert V. 2011 *Phys. Rev. Lett.* **107** 016401
[37] Gatti M, Bruneval F, Olevano V and Reining L 2007 *Phys. Rev. Lett.* **99** 266402
[38] Tomczak J M and Biermann S 2007 *J. Phys.: Condens. Matter* **19** 365206
[39] Grau-Crespo R, Wang H and Schwingenschlogl 2012 *Phys. Rev. B* **86** 081101
[40] Sommers C and Doniach S 1978 *Solid State Commun.* **28** 133
[41] Abdellaoui I, Remli F, Mahmoudi A and Dergal M 2022 *Solid State Commun.* **347** 114710
[42] Mohebbi E, Pavoni E, Mencarelli D, Stipa P, Pierantoni L and Laudadio E 2022 *Nanoscale Adv.* **4** 3634
[43] Kim S, Kim K, Kang C J and Min B I 2013 *Phys. Rev. B* **87** 195106
[44] Kinaci A, Kado M, Rosenmann D, Ling C, Zhu G, Banerjee D and Chan M K 2015 *Appl. Phys. Lett.* **107** 262108
[45] Stahl B and Bredow T 2020 *J. Comput. Chem.* **41** 258

[46] Cococcioni M and De Gironcoli S 2005 *Phys. Rev. B* **71** 035105
[47] Sasoglu E, Friedrich C and Blugel S 2011 *Phys. Rev. B* **83** 121101
[48] Wang Y C and Jiang H 2019 *J. Chem. Phys.* **150** 154116
[49] Sakuma R, Miyake T and Aryasetiawan F 2008 *Phys. Rev. B* **78** 075106
[50] Liu G H, Deng X Y and Wen R 2010 *J. Mater. Sci.* **45** 3270
[51] Budai J D, Hong J, Manley, M E, Specht E D, Li C W, Tischler J Z, Abernathy D L, Said A H, Leu B M, Boatner L A, McQueeney R J and Delaire O 2014 *Nature* **515** 535
[52] Kresse G and Joubert D 1999 *Phys. Rev. B* **59** 1758
[53] Kresse G and Furthmuller J 1996 *Phys. Rev. B* **54** 11169
[54] Blochl P E, Jepsen O and Andersen O K 1994 *Phys. Rev. B* **49** 16223
[55] Perdew J P, Burke K and Ernzerhof M 1996 *Phys. Rev. Lett.* **77** 3865
[56] Togo A and Tanaka I 2015 *Scr. Mater.* **108** 1
[57] Togo A, Chaput L, Tanaka I and Hug G 2010 *Phys. Rev. B* **81** 174301
[58] Baroni S, De Gironcoli S, Dal Corso A and Giannozzi P 2001 *Rev. Mod. Phys.* **73** 515
[59] Baroni S, Giannozzi P and Isaev E 2011 arXiv:1112.4977 [cond-mat.mtrl-sci]
[60] Longo J M, Kierkegaard P, Ballhausen C J, Ragnarsson U, Rasmussen S E, Sunde E and Sorensen N A 1970 *Acta Chem. Scand.* **24** 420
[61] McWhan D B, Marezio M, Remeika J P and Dernier P D 1974 *Phys. Rev. B* **10** 490
[62] Lee S, Hippalgaonkar K, Yang F, Hong J, Ko C, Suh J, Liu K, Wang K, Urban J J, Zhang X, Damnes C, Hartnoll S A, Delaire O and Wu J 2017 *Science* **355** 371
[63] Hua Z W, Zheng T, Sang J X, Xu X F, Wu B H and Wei L F 2021 *J. Phys. D* **54** 355302
[64] Vinet P, Rose J H, Ferrante J and Smith J R 1989 *J. Phys.: Condens. Matter* **1** 1941
[65] Zylbersztejn A and Mott N F 1975 *Phys. Rev. B* **11** 4383
[66] Chandrashekhar G V, Barros H L C and Honig J M 1973 *Mater. Res. Bull.* **8** 369